Extreme Mechanics Letters 53 (2022) 101679

Contents lists available at ScienceDirect

Extreme Mechanics Letters

journal homepage: www.elsevier.com/locate/eml

Fatigue of amorphous hydrogels with dynamic covalent bonds

Yihang Xiao [a,1], Qi Li [a,b,1], Xi Yao [c], Ruobing Bai [d], Wei Hong [a], Canhui Yang [a,*]

[a] Department of Mechanics and Aerospace Engineering, Southern University of Science and Technology, Shenzhen, Guangdong 518055, PR China
[b] State Key Laboratory for Turbulence and Complex Systems, Department of Mechanics and Engineering Science, BIC-ESAT, College of Engineering, Peking University, Beijing 100871, PR China
[c] Key Lab for Special Functional Materials of Ministry of Education, Henan University, Kaifeng 475004, Henan Province, PR China
[d] Department of Mechanical and Industrial Engineering, College of Engineering, Northeastern University, Boston, MA, 02115, USA

ARTICLE INFO

Article history:
Received 10 January 2022
Received in revised form 10 February 2022
Accepted 28 February 2022
Available online 9 March 2022

Keywords:
Hydrogel
Amorphous polymer network
Anti-fatigue
Dynamic covalent bond

ABSTRACT

Hydrogels composed of amorphous polymer networks are widely used as soft and stretchable components in diverse devices and machines. However, existing amorphous hydrogels are susceptible to fatigue fracture. Here, we propose that amorphous hydrogels with dynamic covalent bonds can resist fatigue fracture, so long as the dynamics of bond recovery is faster than the rate of deformation. We examine this hypothesis by performing fatigue tests for polyacrylamide hydrogels crosslinked by covalent C–C bonds and by dynamic covalent siloxane bonds, using N, N'-methylenebis-acrylamide (MBAA) and silanes as the crosslinkers, respectively. Experiments show that the fatigue threshold of MBAA-crosslinked hydrogels is 12.7 J/m^2, much lower than the toughness, 70.2 J/m^2, and comparable to the Lake–Thomas prediction, 11.17 J/m^2, while the silane-crosslinked hydrogels achieve a fatigue threshold of 68.7 J/m^2, surprisingly close to the toughness, 86.2 J/m^2, which is reported for the first time in hydrogels with dynamic covalent bonds. We trace the violation of the Lake–Thomas mechanism to the dynamic nature of siloxane bonds. We carry out self-healing tests, self-recovery tests, and fatigue tests for silane-crosslinked hydrogels with different pH values to examine the bond dynamics. We discuss the importance of dynamic covalent bonds in synthesizing fatigue-free hydrogels by constructing a fatigue threshold-toughness Ashby plot. The current work suggests that dynamic covalent bonds pave alternative avenues towards anti-fatigue soft materials with amorphous polymer networks.

1. Introduction

Hydrogels are aggregations of polymer networks and water. Owing to the unique combination of superior properties, hydrogels have found tremendous applications in biomedicine and engineering, encompassing drug delivery [1], tissue repairing [2–4], wound dressing [5–8], medical implants [9], soft machines [10], soft robotics [11] and ionotronics [12–14].

In many engineering practices, mechanical robustness of a hydrogel is the prerequisite. Particularly, hydrogels are often required to sustain prolonged cyclic loads. Whereas various strong and tough hydrogels have been developed over the past two decades [15–17], most of them are prone to fatigue by degrading mechanical properties or undergoing fatigue fracture [18]. The issue of fatigue greatly impedes the practical applications of hydrogels.

The study of the fatigue of hydrogel is nascent [18]. Immediately after the initiation [19], intensive efforts have been devoted to investigating the fatigue behaviors of various kinds of hydrogels [20–32]. Meanwhile, the uncovered underlying mechanics has facilitated the design and synthesis of tough and fatigue-resistant hydrogels, such as multi-length-scale hierarchical hydrogels [25–29] and composite hydrogels with mitigated stress concentration [30,31]. Despite these exhilarating hydrogels with deliberately architected structures, most hydrogels commonly used in the laboratories worldwide are generally synthesized in more facile manners and composed entirely of amorphous polymer networks. Amorphous polymer networks, as revealed by Lake and Thomas [33], suffer fatigue fracture: the fatigue threshold, that is the minimal energy needed to extend a crack by unit area, is equal to the total bond energy stored in the polymer chains lying across the crack plane, independent of the background energy dissipation. Existing amorphous hydrogels, either single-network or double-network, are reported to be subjected to the same molecular disease without exception [18–23]. Fatigue fracture is plausibly inherent for amorphous hydrogels.

Here we propose that anti-fatigue hydrogels can be achieved with amorphous polymer networks. Without losing generality,

* Corresponding author.
E-mail address: yangch@sustech.edu.cn (C. Yang).
[1] These authors contribute equally to this work.

https://doi.org/10.1016/j.eml.2022.101679
2352-4316/

we assume an amorphous covalent polymer network, in which covalent bonds link monomer units into polymer chains and crosslink polymer chains into a network. Fatigue fracture eventually results from the catastrophic proliferation of network damage, which stems from bond breaking at a crosslink or at a certain bond along a polymer chain. Whereas most cleavages of covalent bonds are irreversible, some covalent bonds are strong yet reversible, e.g. siloxane bonds and disulfide bonds [34]. For an amorphous polymer network consisting of such dynamic covalent bonds, the accumulation or even initiation of damage may be prohibited under certain rate of deformation. With these considerations in mind, we hypothesize that amorphous hydrogels with dynamic covalent bonds can resist fatigue fracture, so long as the dynamics of bond recovery is faster than the rate of deformation. We examine this hypothesis by investigating and comparing the fatigue behaviors of polyacrylamide hydrogels crosslinked by two types of crosslinkers: irreversible covalent C–C bonds using N, N′-methylenebis-acrylamide (MBAA) and reversible dynamic covalent siloxane bonds using silanes. Fatigue fracture tests show that the MBAA-crosslinked hydrogels achieve a fatigue threshold of 12.7 J/m^2, comparable to the Lake–Thomas prediction of 11.17 J/m^2 and much lower than the toughness 70.2 J/m^2, while the silane-crosslinked hydrogels achieve a fatigue threshold of 68.7 J/m^2, surprisingly close to the toughness 86.2 J/m^2. We probe the violation of the Lake–Thomas prediction by examining the dynamics of siloxane bonds through self-healing tests, self-recovery tests, and fatigue tests for silane-crosslinked hydrogels with different pH values. Siloxane bond showcases a potent method to realize amorphous hydrogels of fatigue threshold comparable to toughness. With the abundant chemistry of dynamic bonds, it is expected that more anti-fatigue amorphous hydrogels and other amorphous polymer networks will be designed and synthesized.

2. Proposed mechanism of anti-fatigue

For simplicity, consider a single-network hydrogel of amorphous covalent polymer network. Any rate-dependent processes of viscoelasticity (such as friction between polymer chains or between polymer chains and solvent) or poroelasticity will be neglected. As illustrated in Fig. 1, when a sample of amorphous covalent polymer network containing a crack of length c is loaded, the crack tip concentrates stress and a dissipation zone forms in the vicinity of the crack tip. The polymer chains in the dissipation zone deform more and thus carry more load than the polymer chains in other regions of the sample. When the bond along a polymer chain or at a crosslink is about to break, the associated polymer chains are stretched taut (in red). Upon bond breaking, the stretched polymer chains relax and dissipate all strain energy stored in the entire chains. The amount of energy dissipated depends on the strength of the broken bonds. As a result, entropic polymer chains are molecular-scale elastic dissipaters [35]. Provided an adequately strong elastic backbone, if the bonds along the polymer chain or at the crosslink are reversible, the ruptured polymer network in the fracture process zone can regain its original state statistically after unloading as a result of bond reformation. The sample will behave the same as a pristine one if the reformation of bonds is complete before the next loading. In this sense, the polymer network is anti-fatigue.

3. Selection of materials

To validate our hypothesis, we select the widely used polyacrylamide (PAAm) hydrogel as a model system. In synthesizing PAAm hydrogels, we use two types of crosslinkers: N, N′-methylenebisacrylamide (MBAA) and silane coupling agent (3-(trimethoxysilyl) propyl methacrylate, TMSPMA). Specifically, the

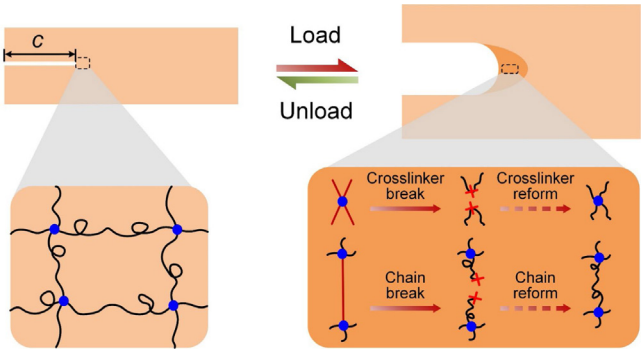

Fig. 1. Anti-fatigue mechanism of an amorphous polymer network with reversible covalent bonds. When an amorphous polymer network containing a crack of length c is loaded, the crack tip concentrates stress, causing the break of either the crosslinks or certain polymer chains within the fracture process zone to dissipate energy. The broken bonds reform after unloading, and the network is anti-fatigue so long as the reforming processes complete before the subsequent loading. The black lines represent stress-free polymer chains, and the red lines represent tightly stretched polymer chains. The solid blue circles represent crosslinks. (For interpretation of the references to color in this figure legend, the reader is referred to the web version of this article.)

pH value of silane-crosslinked hydrogel is tuned to be 2.8 to facilitate the kinetics of silane condensation [36]. MBAA leads to a PAAm network of irreversible covalent crosslinks (Fig. 2a), while TMSPMA leads to a PAAm network of reversible covalent crosslinks (Fig. 2b). In principle, the crosslink resulting from the condensation of two silanol groups is equivalent to the crosslink of one MBAA molecule [37]. Nevertheless, the free radical polymerization and crosslinking of PAAm chains are proceeded randomly, resulting in the deviation from the ideal prediction. For reasonable comparison, in experiments, we adjust the amount of crosslinker while keeping other ingredients of the two hydrogels identical, such that, under affine deformation, the nominal stresses in the two types of hydrogels are nearly the same, even under fatigue loads. After optimizations following this principle, we set the weight ratios of MBAA and TMSPMA with respect to monomer as 0.0026 and 0.037, respectively. We measure the nominal stress–stretch curves of the two types of hydrogels by cyclic pure shear tests (Fig. 2c & d). The stress–stretch curves of the two hydrogels are close to each other in the first loading cycle. In subsequent cycles, the MBAA-crosslinked hydrogel exhibits a slight softening phenomenon and reaches a steady state after 100 cycles, while the silane-crosslinked hydrogel exhibits more obvious softening and reaches a steady state after 1000 cycles, aside from the non-recoverable deformation. Regardless of this difference, the mechanical properties and responses (e.g. shear modulus and peak stress) of the two hydrogels at their steady states become even closer to each other.

4. Fatigue damage tests

In general, fatigue is studied through two types of tests: fatigue damage test using unnotched samples and fatigue fracture test using notched samples [24]. We first characterize the fatigue damage properties of the two hydrogels using pure shear test (Fig. 3a). Fig. 3b exemplifies a sample elongated to a stretch of $\lambda = 1.6$. We collect the evolution of nominal stress–stretch curves of MBAA-crosslinked PAAm hydrogel (Fig. 3c) and silane-crosslinked PAAm hydrogel (Fig. 3d) over cycles. MBAA-crosslinked hydrogels exhibit nearly elastic behaviors with tiny hysteresis, while silane-crosslinked hydrogels undergo a slight shakedown (namely the stress becomes smaller compared to that of pristine sample at the same stretch) and exhibit obvious hysteresis. The slight shakedown might be ascribed to the inevitable

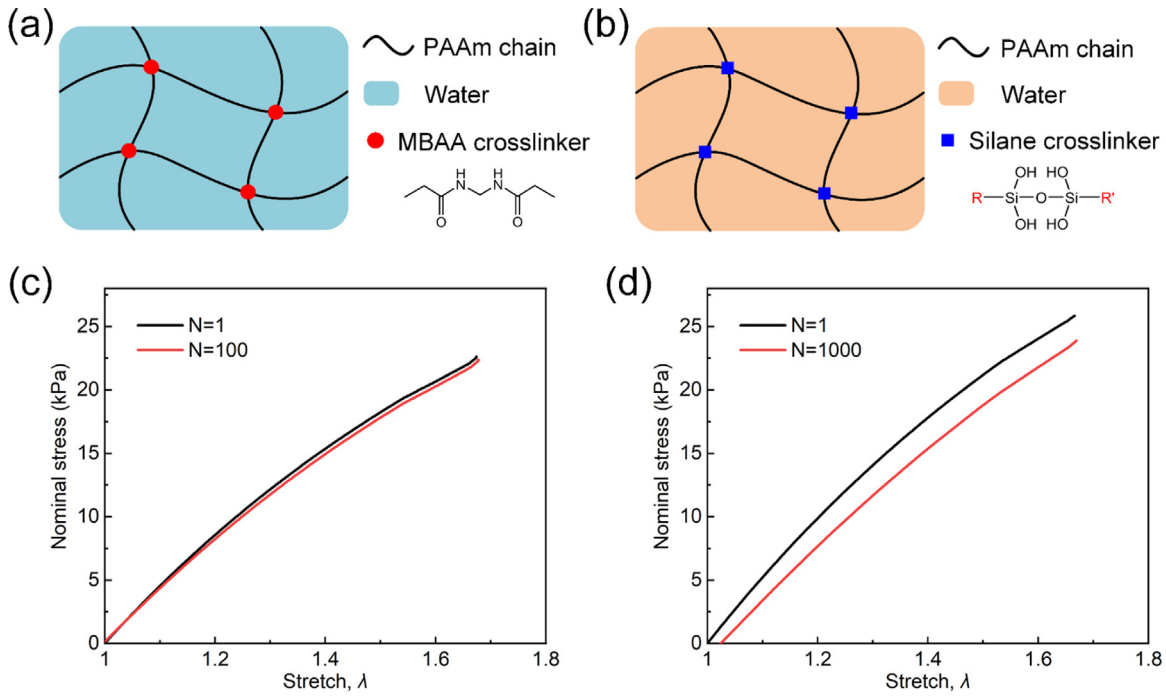

Fig. 2. Schematics of two types of PAAm hydrogels and their nominal stress–stretch curves. (a) MBAA-crosslinked PAAm hydrogel. (b) Silane-crosslinked PAAm hydrogel. Nominal stress–stretch curves for (c) MBAA-crosslinked hydrogel at 1st and 100th cycles, and (d) silane-crosslinked hydrogel (pH = 2.8) at 1st and 1000th cycles.

scission of polymer chains due to network imperfection [38]. Besides, the dynamic breaking and reforming of siloxane bonds might facilitate the rearrangement of the conformation of the polymer network to alleviate stress. On the other hand, the finite hysteresis is persistent, implying the existence of reversible energy dissipation. Since the MBAA-crosslinked hydrogel has negligible hysteresis, we ascribe the persistent hysteresis of silane-crosslinked hydrogel to the dynamic breaking and reforming of siloxane bonds.

To characterize and compare the fatigue damage of the two types of hydrogels more quantitatively, we extract the shear modulus and peak stress as functions of the number of cycles from the nominal stress–stretch curves. According to the neo-Hookean model [39], under pure shear configuration, the nominal stress σ is related to the stretch λ as

$$\sigma = \mu(\lambda - 1/\lambda^3), \tag{1}$$

where μ is the shear modulus and considered as an invariant. By fitting the experimental data, the shear modulus at each cycle is obtained and plotted against the number of cycles (Fig. 3e). After slight initial declines, the shear moduli of both hydrogels remain unchanged over cycles and, more importantly, converge to the same values. Similar tendency is observed for the peak stress (Fig. 3f). Thus, both MBAA-crosslinked PAAm hydrogel and silane-crosslinked PAAm hydrogel are resistant to fatigue damage.

5. Fatigue fracture tests

We next perform fatigue fracture tests to measure the fatigue threshold. An edge notch of 20 mm is precut along the center line of each sample (Fig. 4a). A sample is taken to be free of fatigue fracture if no noticeable crack propagation is detected after 30000 cycles. The crack growth Δc as a function of the number of cycle N is plotted for MBAA-crosslinked hydrogel in Fig. 4b and silane-crosslinked hydrogel in Fig. 4c. After an initial fluctuation, the crack extension reaches a steady state, where Δc increases with the number of cycles approximately in a linear manner. For the pure shear configuration, the applied stretch λ relates to the energy release rate G as [40]

$$G = W(\lambda)\, h_0, \tag{2}$$

where h_0 is the height of sample measured in the undeformed state, and $W(\lambda)$ is the elastic strain energy per unit volume and calculated as $W(\lambda) = \int_1^\lambda \sigma(\lambda) d\lambda$, where the corresponding nominal stress–stretch curve measured on an unnotched sample (e.g., from the fatigue damage test) is used for the integration. When the sample fractures at the first cycle, the test gives the toughness, or fracture energy, of the hydrogel. The toughness is 70.2 J/m^2 for the MBAA-crosslinked hydrogel and is 86.2 J/m^2 for the silane-crosslinked hydrogel.

By fitting the crack growth Δc to a linear function of N in the steady state, crack extension per cycle dc/dN versus energy release rate G can be obtained (Fig. 4d). dc/dN is zero at a relatively low G. Above a certain critical G, dc/dN increases with G. We conduct linear regression to the data beyond the critical point and set the interception with the G axis as the fatigue threshold, Γ_{th}, below which the crack does not propagate. The fatigue threshold is 68.7 J/m^2 for silane-crosslinked hydrogel (pH = 2.8) and is 12.7 J/m^2 for MBAA-crosslinked hydrogel. For the MBAA-crosslinked hydrogel, no crack extension is observed after 30000 cycles at G = 12.7 J/m^2 (Fig. 5a), whereas the crack grows by 30.8 mm after 15000 cycles at G = 24.5 J/m^2 (Fig. 5b). For the silane-crosslinked hydrogel, no crack extension is observed after 30000 cycles at G = 68.7 J/m^2 (Fig. 5c), whereas the crack propagates slightly at G = 75.3 J/m^2 (Fig. 5d). The fatigue threshold of silane-crosslinked hydrogel is surprisingly close to the toughness and is much higher than that of MBAA-crosslinked hydrogel.

Following the Lake–Thomas model [33], the fatigue threshold of a covalently crosslinked, amorphous, single-network hydrogel can be estimated by

$$\Gamma_{th} = \phi_p b U l \sqrt{n}, \tag{3}$$

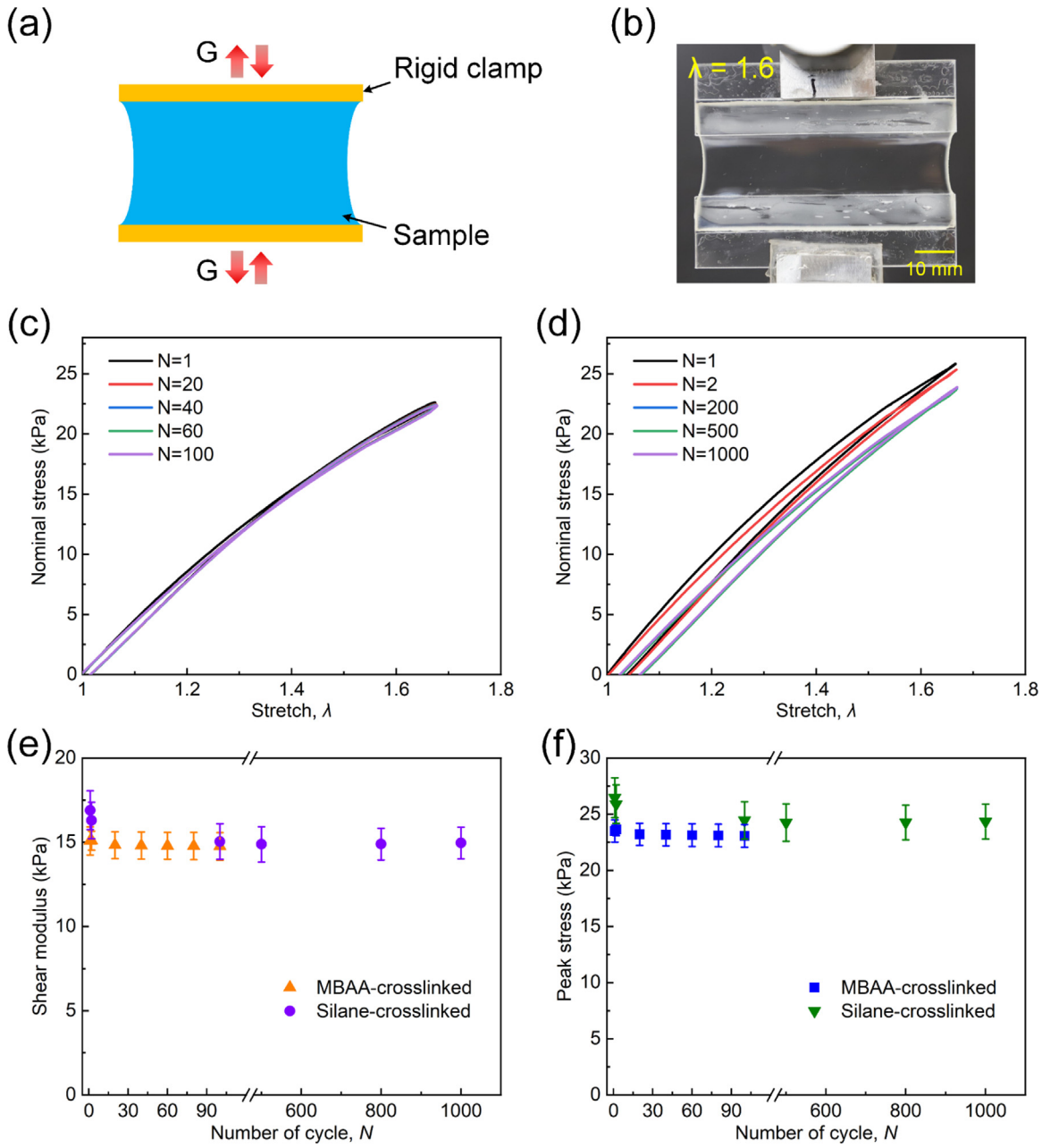

Fig. 3. Fatigue damage characterizations. (a) Schematic of fatigue damage test. (b) Digital image of a stretched silane-crosslinked hydrogel sample at $\lambda = 1.6$. Cyclic nominal stress–stretch curves for (c) MBAA-crosslinked and (d) silane-crosslinked (pH = 2.8) PAAm hydrogels. (e) Shear modulus, and (f) peak stress as a function of the number of cycles.

where ϕ_p is the volume fraction of the polymer in the hydrogel, b is the number of C–C bonds per unit volume of polymer, U is the chemical energy of a single C–C bond, l is the length of repeat unit, and n is the number of repeat unit between two crosslinks. n can be calculated by

$$n = n_{AAm}/N, \tag{4}$$

where n_{AAm} is the number of monomers per unit volume of polymer, and N is the number of chains per unit volume of polymer. Whereas N can be calculated theoretically, here we estimate the value of N based on experimental measurements. Recall that the shear modulus μ of hydrogel can be determined as [41]

$$\mu = \phi_p^{1/3} NkT, \tag{5}$$

where kT is the absolute temperature in unit of energy. Our recipe gives $\phi_p = 20.5\%$. Other parameters are taken as $b \approx n_{AAm} = 9.32 \times 10^{27}/\mathrm{m}^3$, $U = 3.3 \times 10^{-19}$J, $l \approx b^{-1/3} = 4.75 \times 10^{-10}$m, and $kT = 4.11 \times 10^{-21}$J. Once the shear modulus of hydrogel is determined from the nominal stress–stretch curve, the fatigue threshold of hydrogel can be obtained by solving Eqs. (3)–(5). For the MBAA-crosslinked hydrogel, Γ_{th} is estimated as 11.17 J/m^2, comparable to the experimental result, 12.7 J/m^2. However, for the silane-crosslinked hydrogel, Γ_{th} is estimated as 11.01 J/m^2, much lower than the experimental result, 68.7 J/m^2. For the first time, we report the violation of the Lake–Thomas picture in covalently crosslinked, amorphous, single-network hydrogels.

6. Anti-fatigue mechanism of silane-crosslinked hydrogel

The agreement between the measured and the Lake–Thomas predicted fatigue thresholds of the MBAA-crosslinked PAAm hydrogel has been appreciated before [18]. However, what causes

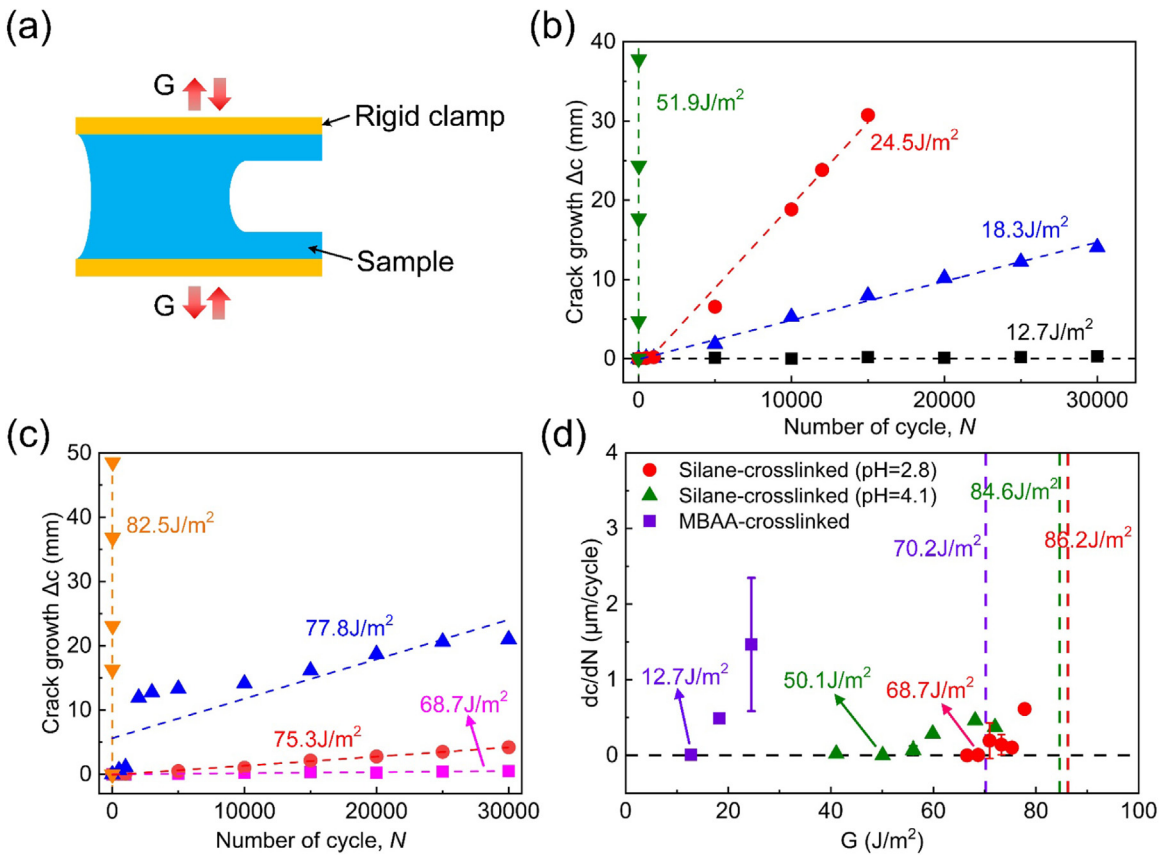

Fig. 4. Fatigue fracture characterizations. (a) Schematic of fatigue fracture test. Crack growth as a function of the number of cycles for (b) MBAA-crosslinked and (c) silane-crosslinked (pH = 2.8) PAAm hydrogels. (d) Crack growth rate dc/dN as a function of G for MBAA-crosslinked and silane-crosslinked (pH = 2.8 and pH = 4.1) PAAm hydrogels. (For interpretation of the references to color in this figure legend, the reader is referred to the web version of this article.)

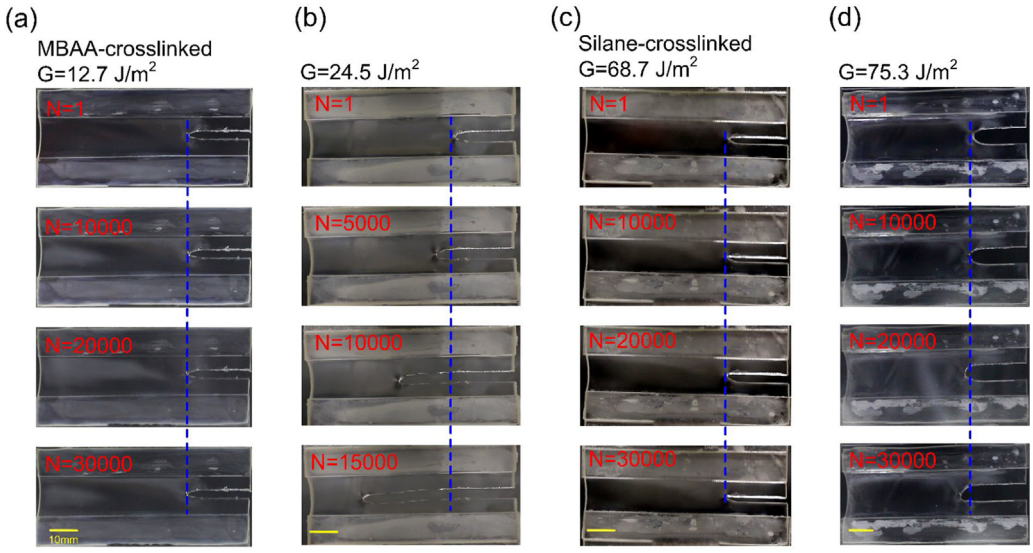

Fig. 5. Snapshots showing the crack propagation during fatigue fracture tests. Precut MBAA-crosslinked PAAm hydrogels at various numbers of cycle under applied energy release rate of (a) 12.7 J/m^2 and (b) 24.5 J/m^2. Precut silane-crosslinked PAAm hydrogels (pH = 2.8) at various numbers of cycle under applied energy release rate of (c) 68.7 J/m^2 and (d) 75.3 J/m^2.

the large discrepancy in the measured fatigue threshold of the silane-crosslinked PAAm hydrogel from the Lake–Thomas prediction? Since the two types of hydrogels have identical compositions except the crosslinks and have near-identical mechanical responses under affine deformation, we attribute the breakdown of the Lake–Thomas mechanism in the silane-crosslinked hydrogel to the dynamic nature of siloxane bonds. The mechanism is proposed as following. As schematized in Fig. 6a, the chemical bonds in both backbones and crosslinks of a MBAA-crosslinked PAAm hydrogel are C–C bonds, which do not reform after break. By contrast, the chemical bonds at crosslinks in a silane-crosslinked PAAm hydrogel are Si–O–Si bonds (Fig. 6b).

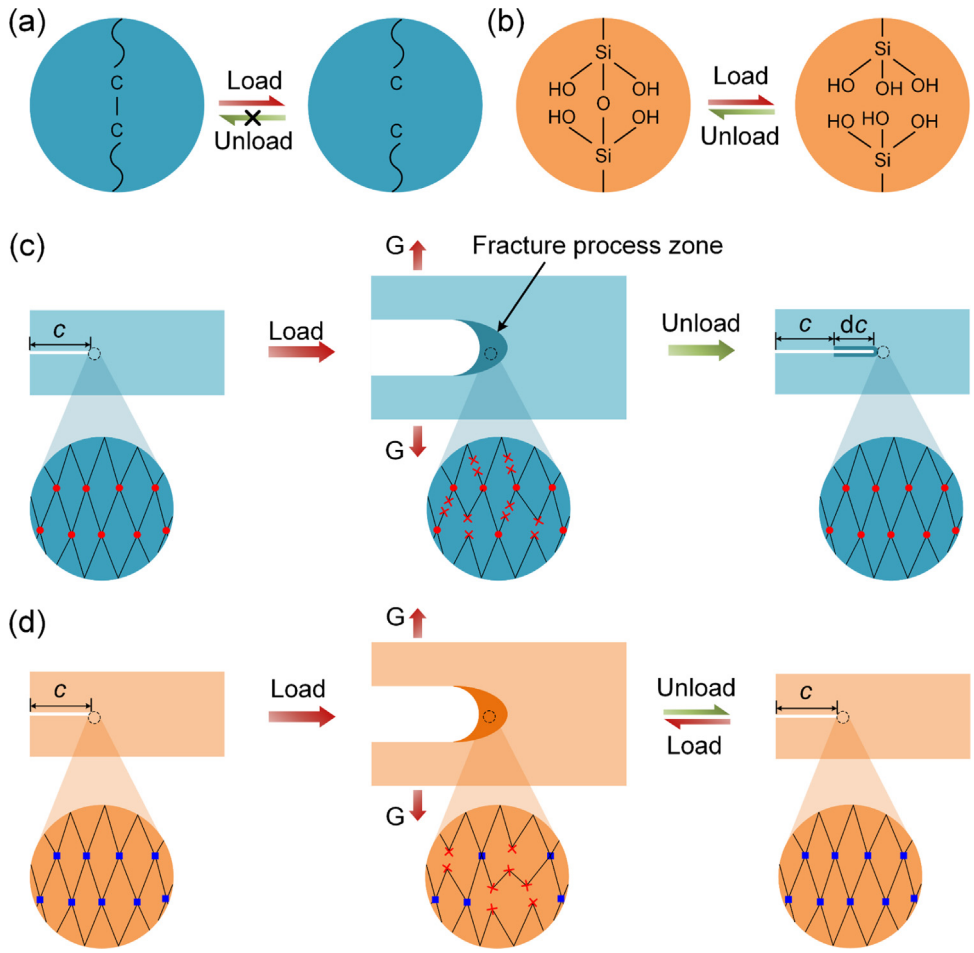

Fig. 6. Fatigue mechanism of MBAA-crosslinked hydrogel and anti-fatigue mechanism of silane-crosslinked hydrogel. (a) The breaking of C–C bond in MBAA-crosslinked hydrogel is irreversible. (b) The breaking of Si–O–Si bond in silane-crosslinked hydrogel is reversible. (c) Under cyclic load, the polymer chains in the fracture process zone of MBAA-crosslinked hydrogel gradually break, causing the crack to extend cycle by cycle. (d) Under cyclic load, the siloxane bonds in the fracture process zone break and reform repeatedly, dissipating energy without crack propagation.

The breaking of Si–O–Si bonds is reversible, following Si–O–Si + $H_2O \rightleftarrows$ 2Si–OH. When a precut MBAA-crosslinked PAAm hydrogel is loaded, the crack opens, and a fracture process zone emerges in front of the crack tip (Fig. 6c). Within the fracture process zone, irreversible chain scission occurs and the crack extends once all polymer chains in front of the crack tip break. New crack tip forms subsequently and the above process repeats until the ultimate fracture of the sample. When a silane-crosslinked PAAm hydrogel containing an edge crack is loaded, the Si–O–Si bonds within the fracture process zone break to dissipate energy (Fig. 6d). However, the Si–O–Si bonds can reform fast adequately after unloading, such that the network within the fracture process zone heals and regains load-carrying capability before the subsequent loading. The breaking and reforming of Si–O–Si bonds ensue periodically to resist crack propagation.

7. Self-healing and self-recovery tests

Our proposed mechanism is based on the postulate that the siloxane bonds are reversible within the time scale of each loading cycle. To verify the reversibility of siloxane bonds, we conduct self-healing and self-recovery tests for the silane-crosslinked PAAm hydrogel (pH = 2.8). For self-healing test, we prepare rectangular samples, with sizes of 50 mm in length, 10 mm in width and 3 mm in thickness, cut each sample into two pieces and attach the freshly cut surfaces with each other seamlessly afterwards. For a healing time of 4 hours, the healed sample can sustain a tensile stretch of $\lambda = 1.33$ before fracture (Fig. 7a), whereas the sample without healing cannot even sustain its own weight. The uniaxial nominal stress–stretch curves of samples with different healing times are shown in Fig. 7b. The maximum stretch to rupture and strength of healed samples increase with healing time, but are much lower than those of pristine samples. This is not surprising since cutting breaks not only the siloxane bonds, but also the C–C bonds, which account for the majority of broken bonds yet cannot heal. We plot the heal efficiency, defined as the peak stress of the healed sample divided by that of the pristine sample, and the shear modulus against the healing time (Fig. 7c). The healing efficiency increases with the healing time then plateaus and maximizes at ∼40%. Interestingly, for different healing times tested in our experiments, the shear moduli of all healed samples are very close to that of pristine sample. The reason is that the shear modulus is a macroscopic parameter, mainly determined by the polymer chains in the bulk through the entropic elasticity. Such bulk property is barely affected by the cut as long as the healed surface, which is in series with the remaining bulk, is strong enough to bear a finite load.

We characterize the self-recovery behaviors of silane-crosslinked hydrogel under fatigue damage conditions using pure shear specimens. Certain degree of shakedown sets in Fig. 7d. After recovery, the nominal stress–stretch curve (purple curve in Fig. 7d) almost coincides with that in the first cycle (black curve in Fig. 7d), implying a near-perfect recovery. Put together, self-healing and self-recovery tests confirm the reversibility of siloxane bonds.

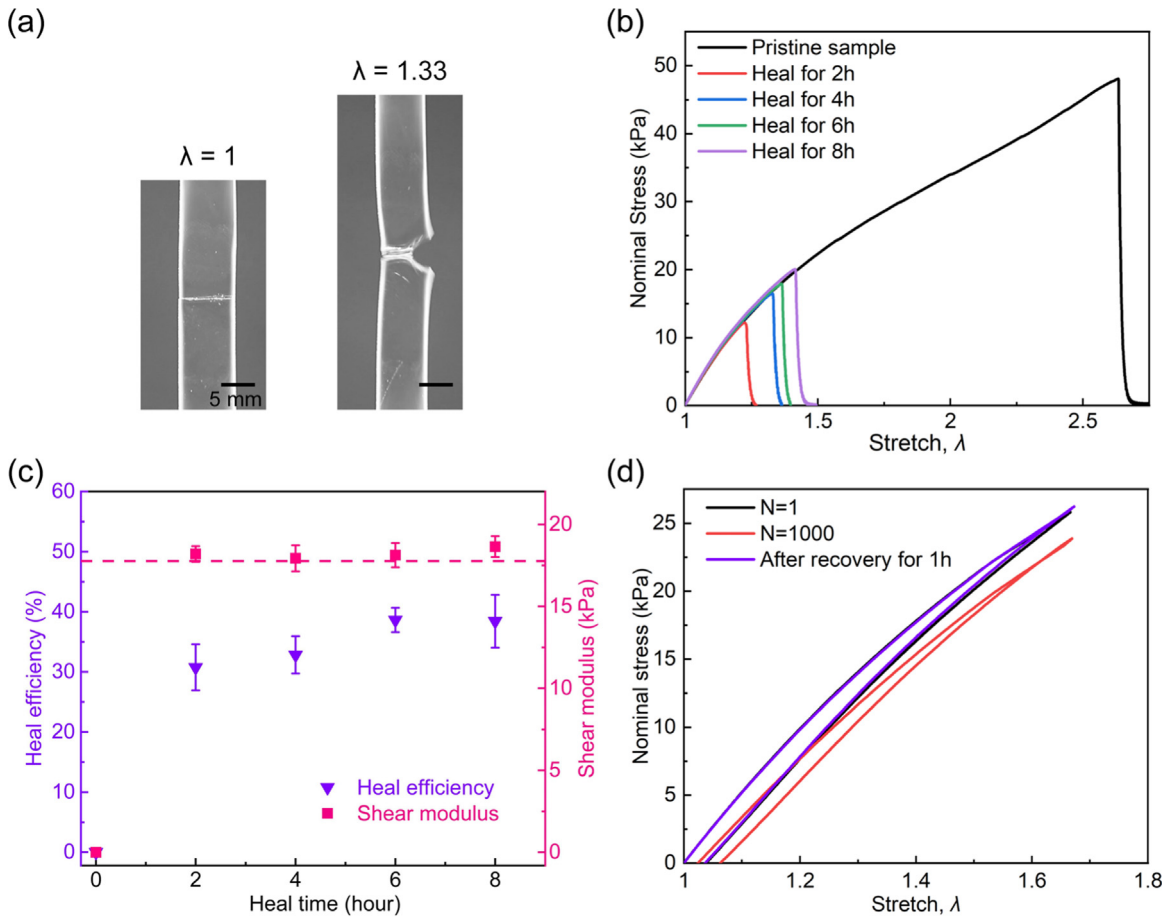

Fig. 7. Self-healing and self-recovery tests of silane-crosslinked PAAm hydrogel (pH = 2.8). (a) A piece of rectangular-shaped sample, cut and then healed for 4 hours at room temperature, can be stretched to $\lambda = 1.33$ before rupture. (b) Nominal stress–stretch curves of pristine and healed samples with different healing times. (c) Heal efficiency and the shear modulus as a function of healing time. The dash line indicates the shear modulus of the pristine sample. (d) Cyclic nominal stress–stretch curves at 1st, 1000th cycles and after recovery for 1 hour at room temperature. (For interpretation of the references to color in this figure legend, the reader is referred to the web version of this article.)

8. Fatigue of silane-crosslinked hydrogels with different pH values

Our hypothesis also entails that the dynamics of siloxane bonds is faster than the rate of deformation. To test the validity of this assumption, we synthesize silane-crosslinked hydrogels with different pH values and investigate their fatigue behaviors. The kinetics of silane condensation process is known to be sensitive to pH, with the lowest condensation rate occurring around pH = 4 [36,37]. So far we have been using a pH value of 2.8. Now we prepare hydrogels with pH = 4.1 and conduct fatigue fracture tests to measure the fatigue threshold (Fig. 8a). Fig. 8b shows that no crack extension is observed after 30000 cycles at $G = 41.07$ J/m^2, while the crack grows slightly after 30000 cycles at $G = 59.86$ J/m^2. The dc/dN versus G data are collected in Fig. 4d (green color). The fatigue threshold (50.1 J/m^2) is lower than the fracture toughness (84.6 J/m^2), but is still much higher than the Lake–Thomas prediction. Comparing the silane-crosslinked hydrogels with pH = 2.8 and pH = 4.1, the two hydrogels possess comparable toughness but different fatigue thresholds (68.7 J/m^2 vs 50.1 J/m^2), where the threshold at pH = 2.8 is considerably higher than the fatigue threshold at pH = 4.1. Indeed, the hydrogel with slower silane condensation rate has lower fatigue threshold, consistent with our assumption: in the case of pH = 4.1, less crosslinks in the fracture process zone are able to completely heal within the time scale of one loading cycle thus dissipating less energy and less resisting crack growth. Similarly, in the self-healing test, the hydrogel with pH = 4.1 exhibits increasing healing efficiency but mostly constant shear modulus with healing time (Fig. 8c). In the self-recovery test, the hydrogel restores mechanical properties after 1 hour (Fig. 8d). These results further suggest that anti-fatigue behavior depends on the dynamics of siloxane bonds.

9. Fatigue threshold-toughness Ashby plot

In many engineering applications, hydrogels need to bear prolonged cyclic loads or deformation. In developing hydrogels for such scenarios, both toughness, the resistance to crack growth under monotonic load, and fatigue threshold, the resistance to crack growth under cyclic load, are of central importance. Whereas many methods have been developed to enhance the toughness of hydrogels [15–17], they fail in or do not suit for enhancing the fatigue threshold of amorphous hydrogels. We collect the toughness and fatigue threshold of various hydrogels from recent literatures and plot them in the fatigue threshold-toughness Ashby plot (Fig. 9). The diagonal dash line represents equivalent toughness and fatigue threshold of a hydrogel, which is called fatigue-free. A fatigue-free hydrogel typically does not have potent energy dissipation. Notably, the silane-crosslinked PAAm hydrogels synthesized in this work (solid brown hexagons), especially the hydrogels with pH = 2.8, locate very close to the diagonal. Most existing hydrogels are fatigue-prone, with the fatigue threshold much lower than the toughness, occupying the

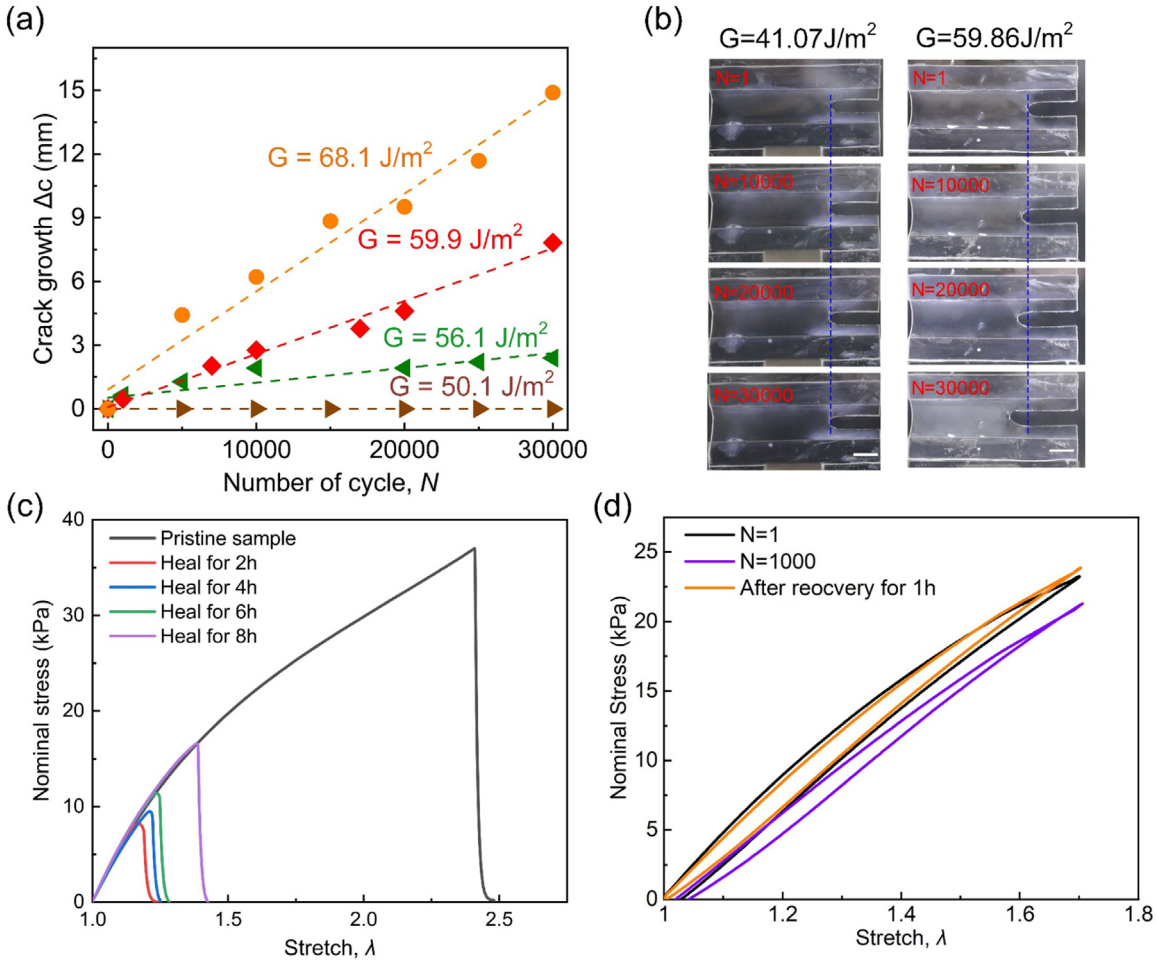

Fig. 8. Fatigue fracture, self-healing and self-recovery tests of silane-crosslinked PAAm hydrogel with pH = 4.1. (a) Crack growth as a function of the number of cycles at different energy release rates. The corresponding dc/dN vs G curve is plotted in Fig. 4d (green color). (b) The propagation of crack under applied energy release rate of 41.07 J/m^2 and 59.86 J/m^2. (c) Nominal stress–stretch curves of pristine and healed samples with different healing times. (d) Cyclic nominal stress–stretch curves at 1st, 1000th cycles and after recovery for 1 hour at room temperature.

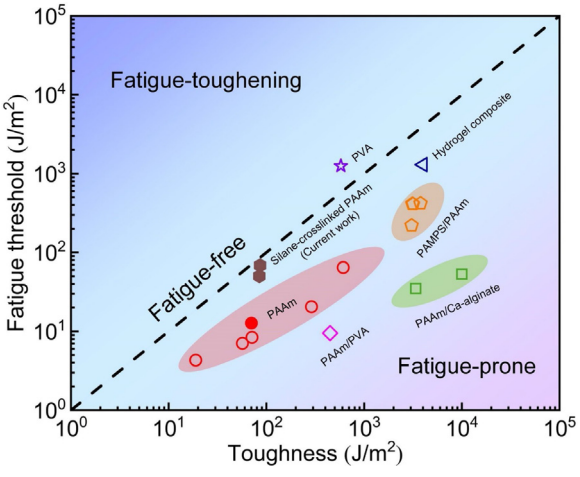

Fig. 9. Ashby plot of fatigue threshold versus toughness. The diagonal dash line represents materials having equal toughness and fatigue threshold. The hollow data points are collected from literatures: PAAm hydrogels [19,21], PAAm/PVA hydrogels [24], PAAm/Ca-alginate hydrogels [20,22], hydrogel composite [30], PVA hydrogels (the toughness is unpublished and is courtesy of the first author) [25] and PAMPS/PAAm double-network hydrogels [23]. The solid data points represent the measurements in this work.

bottom-right region of the plot. The MBAA-crosslinked PAAm hydrogels as studied in this work (solid red circle), are fatigue-prone. Some other hydrogels such as hydrogel composites, are also almost fatigue-free, benefiting from their heterogeneous structures [23,30]. Above the diagonal, the fatigue threshold is higher than the toughness, implying that the materials do not fatigue but are even toughened over cyclic loads. Hydrogels of such behaviors are called fatigue-toughening. A salient example is human muscle. Whereas recent attempts have been taken in hydrogels to mimic this fatigue behavior of muscles via mechanical training [25,42], such a fascinating feature remains largely inaccessible for most synthetic hydrogels.

10. Discussions

For a MBAA-crosslinked PAAm hydrogel, the polymer network inevitably consists of polymer chains of distributed chain lengths [35]. The short chains will break before the long chains under deformation. The short chains are toughners. Since the scission of short chains is irreversible, the fatigue threshold is lower than the toughness by one to two orders of magnitude. For a silane-crosslinked PAAm hydrogel, the distribution of chain length also exists, but the scission of crosslink is reversible, such that the fatigue threshold is comparable to the toughness. The remaining smaller difference between the fatigue threshold and the toughness might be caused by the distributed irreversible

chain scissions of C–C bonds. In addition, bond exchange is highly possible during the breaking and reforming of siloxane bonds in the fracture process zone: the two silanol groups resulting from the dissociation of a siloxane bond may condensate with other adjacent silanol groups resulting from the dissociation of other siloxane bonds. Due to the large local tensile stretch, the effective polymer chain length between the newly formed crosslinks may increase to alleviate the tensile stress in the reconstructed polymer network. This reconstruction of polymer network generates a "soft" zone in front of the crack tip to shield crack propagation. A similar shielding effect has recently been reported to resist fatigue crack propagation in thermoplastic polyurethanes, although the reorganization at crack tip results in the reinforcement of local polymer network [43].

The dissociation and reassociation of siloxane bonds will reach a state of dynamic equilibrium after many cycles of loads. However, the applied tensile stress will favor the dissociation of siloxane bonds by lowering the energy barrier for bond dissociation [44]. Under a load, dissociation overwhelms condensation to engender excessive silanol groups. Such stress-assist dissociation of siloxane bonds has long been noted especially in the presence of water molecules, e.g. in the fatigue of glass [45], and has been recently reported in the crack extension of a silicone network subjected to a static load [46]. Under cyclic loads, it is possible that the backbone polymer matrix springs back when the material is unloaded in each cycle, to facilitate the condensation between nearby silanol groups to heal the crosslinks.

The bulk of silane-crosslinked PAAm hydrogel has low hysteresis, and the stretch in the bulk polymer network is much lower than the local stretch near the crack tip. Therefore, the enhancement of fatigue threshold is mainly contributed from the processes inside the fracture process zone. Such near-crack strengthening effect has been recently recognized in highly entangled elastomeric polymer networks [47,48]. Whereas we have applied a relatively high macroscopic strain rate, 6 s^{-1}, and the strain rate at crack tip is even higher, we conjecture that the condensation kinetics of silanes were always faster than the rate of deformation, as suggested by our experimental results.

11. Conclusion

In summary, we report that anti-fatigue amorphous hydrogels can be achieved based on dynamic covalent bonds by taking a silane-crosslinked PAAm hydrogel as an example. The silane-crosslinked hydrogel (pH = 2.8) possesses a fatigue threshold of 68.7 J/m^2, abnormally close to the toughness, 86.2 J/m^2, and much higher than the Lake–Thomas prediction, 11.01 J/m^2. The violation of Lake–Thomas picture is attributed to the dynamics of siloxane bonds, which is supported by the results of self-healing and self-recovery tests of the hydrogels, as well as the same characterizations of a hydrogel with a different pH. Dynamic covalent bonds provide a potent mechanism to design and synthesize anti-fatigue amorphous polymer networks.

12. Experimental section

Materials

All chemicals were purchased and used without further purification. We purchased from Aladdin the following substances: monomer acrylamide (AAm, A108465), crosslinker N, N′-Methylenebis (acrylamide) (MBAA, M128783), crosslinker 3-(Trimethoxysilyl) propyl methacrylate (TMSPMA, S111153), and initiator α-ketoglutaric acid (K105571).

Synthesis of silane-crosslinked PAAm hydrogel

Acrylamide powders (28.432 g) were first dissolved in deionized (DI) water (100 mL), then 1 mL TMSPMA and 4 mL α-ketoglutaric acid (0.1 mol L^{-1}) were added to form the hydrogel precursor. The pH value of the precursor was measured as 2.8. The precursor was poured into a reaction mold, made of two parallel glass sheets (20 × 20 mm [2]) with an intervening silicone spacer (3 mm thick). The mold was positioned under an ultraviolet (UV) lamp (15 W 365 nm; UVP XX-15BLB) for 12 hours. After curing, the sample was stored in an oven at 65 °C for 12 hours to allow the silanes to condensate completely. The sample was stored in a plastic bag to prevent dehydration before tests. For the silane-crosslinked PAAm hydrogel with pH = 4.1, the synthetic procedure is same as before except that 0.1184 g sodium hydroxide (NaOH) and 1.21 g glacial acetic acid (CH_3COOH) were added for forming the hydrogel precursor. The pH value of as-prepared precursor was measured as 4.1.

Synthesis of MBAA-crosslinked PAAm hydrogel

Acrylamide powders (28.432 g) were first dissolved in DI water (100 mL), and then 4.8 mL MBAA (0.1 mol L^{-1}) and 4 mL α-ketoglutaric acid (0.1 mol L^{-1}) were added. The precursor was poured into a reaction mold, made of two parallel glass sheets (20 × 20 mm [2]) with an intervening silicone spacer (3 mm thick), followed by illuminating UV light for 2 hours.

Mechanical characterizations

To characterize the fatigue damage properties of hydrogels, unnotched pure shear specimens (70 × 10 × 3 mm [3]) were used. Samples were glued to rigid clamps (acrylate plates) at the top and bottom, and then fixed onto a mechanical test machine (Instron 5966, 100 *N* load cell). We programmed a displacement-controlled triangular loading profile with maximum stretch λ = 1.65 and a constant speed of 15 mm/s. The maximum stretch 1.65 is close to the rupture stretch and is large enough to calculate the energy release rate in fatigue fracture test. The tests were carried out in ambient air at room temperature and the duration of each test was less than 20 min. The weight loss of all samples is measured to be less than 2% after the test.

To characterize the fatigue fracture properties of hydrogels, pure shear specimens (70 × 10 × 3 mm [3]) with a 20 mm-long edge crack were used. The tests were conducted using a dynamic and fatigue testing system (Instron ElectroPuls E3000, 250 *N* load cell). A digital camera (Canon, EOS 6D Mark II) was used to record the evolution of crack propagation. We programmed a displacement-controlled loading profile with a constant speed of 60 mm/s. To prevent the dehydration of hydrogels, the specimens were sealed in a customized chamber which is connected to a humidifier. The weight loss of all samples was measured to be less than 2% after the test.

Self-healing and self-recovery tests

To characterize the self-healing behaviors of silane-crosslinked PAAm hydrogel, rectangle samples with size of 10 × 50 × 3 mm [3] were prepared and stored in plastic bag to prevent dehydration of hydrogels before test. Each sample was cut into two pieces, each had a length of 25 mm, and then attached with each other seamlessly. After being stored for 0 hours, 2 hours, 4 hours, 6 hours, 8 hours, the healed specimens were subjected to tensile test to obtain their stress–stretch curves. The samples with 0 hours healing time are the samples

without healing. The tests were performed using a mechanical test machine with a constant tensile speed of 3 mm/s.

To characterize the self-recovery behaviors of silane-crosslinked PAAm hydrogel, pure shear specimens ($70 \times 10 \times 3$ mm [3]) without precut crack were used. Samples were consecutively stretched and released from $\lambda = 1$ to $\lambda = 1.7$ for 1000 cycles with a displacement-controlled triangular loading profile with a constant speed of 15 mm/s. After the 1000th loading cycle, samples were sealed in plastic bags for recovery for 1 hour. Afterwards, the recovered sample was subjected to one more loading cycle. Nominal stress–stretch curve of 1001th cycle is recorded and compared to the that of 1st and 1000th cycles.

Declaration of competing interest

The authors declare that they have no known competing financial interests or personal relationships that could have appeared to influence the work reported in this paper.

Acknowledgment

The work at Southern University of Science and Technology is supported by Natural Science Foundation of Guangdong Province (2214050008118), and the Centers for Mechanical Engineering Research and Education at Massachusetts Institute of Technology and Southern University of Science and Technology. W. H. acknowledges the financial support from the National Natural Science Foundation of China through Grant 11972015. X. Y. acknowledges the financial support from the National Natural Science Foundation of China through Grant (22172045, 21905077). R.B. acknowledges the startup fund from Northeastern University, China. The authors thank Dr. Shaoting Lin for providing the unpublished data of the toughness of PVA hydrogels.

References

[1] J. Li, D.J. Mooney, Designing hydrogels for controlled drug delivery, Nature Rev. Mater. 1 (12) (2016).
[2] B. Sharma, S. Fermanian, M. Gibson, S. Unterman, D.A. Herzka, B. Cascio, J. Coburn, A.Y. Hui, N. Marcus, G.E. Gold, J.H. Elisseeff, Human cartilage repair with a photoreactive adhesive-hydrogel composite, Sci. Transl. Med. 5 (167) (2013) 167ra6.
[3] J. Li, A. Celiz, J. Yang, Q. Yang, I. Wamala, W. Whyte, B. Seo, N. Vasilyev, J. Vlassak, Z. Suo, Tough adhesives for diverse wet surfaces, Science 357 (6349) (2017) 378–381.
[4] K. Liu, H. Yang, G. Huang, A. Shi, Q. Lu, S. Wang, W. Qiao, H. Wang, M. Ke, H. Ding, T. Li, Y. Zhang, J. Yu, B. Ren, R. Wang, K. Wang, H. Feng, Z. Suo, J. Tang, Y. Lv, Adhesive anastomosis for organ transplantation, Bioactive Mater. (2021).
[5] P.J.M. Bouten, M. Zonjee, J. Bender, S.T.K. Yauw, H. van Goor, J.C.M. van Hest, R. Hoogenboom, The chemistry of tissue adhesive materials, Prog. Polym. Sci. 39 (7) (2014) 1375–1405.
[6] H. Yuk, C.E. Varela, C.S. Nabzdyk, X. Mao, R.F. Padera, E.T. Roche, X. Zhao, Dry double-sided tape for adhesion of wet tissues and devices, Nature 575 (7781) (2019) 169–174.
[7] S. Nam, D. Mooney, Polymeric tissue adhesives, Chem. Rev. 121 (18) (2021) 11336–11384.
[8] Y. Gao, X. Han, J. Chen, Y. Pan, M. Yang, L. Lu, J. Yang, Z. Suo, T. Lu, Hydrogel–mesh composite for wound closure, Proc. Natl. Acad. Sci. 118 (28) (2021).
[9] S.Y. Chin, Y.C. Poh, A.-C. Kohler, J.T. Compton, L.L. Hsu, K.M. Lau, S. Kim, B.W. Lee, F.Y. Lee, S.K. Sia, Additive manufacturing of hydrogel-based materials for next-generation implantable medical devices, Sci. Robot. 2 (2) (2017).
[10] X. Liu, J. Liu, S. Lin, X. Zhao, Hydrogel machines, Mater. Today 36 (2020) 102–124.
[11] Y. Lee, W.J. Song, J.Y. Sun, Hydrogel soft robotics, Mater. Today Phys. 15 (2020).
[12] C. Keplinger, J.-Y. Sun, C.C. Foo, P. Rothemund, G.M. Whitesides, Z. Suo, Stretchable, transparent, ionic conductors, Science 341 (6149) (2013) 984–987.
[13] C. Yang, Z. Suo, Hydrogel ionotronics, Nature Rev. Mater. 3 (6) (2018) 125.
[14] C. Yang, S. Cheng, X. Yao, G. Nian, Q. Liu, Z. Suo, Ionotronic luminescent fibers, fabrics, and other configurations, Adv. Mater. 32 (47) (2020) e2005545.
[15] J.P. Gong, Y. Katsuyama, T. Kurokawa, Y. Osada, Double-Network hydrogels with extremely high mechanical strength, Adv. Mater. 15 (14) (2003) 1155–1158.
[16] J.Y. Sun, X. Zhao, W.R. Illeperuma, O. Chaudhuri, K.H. Oh, D.J. Mooney, J.J. Vlassak, Z. Suo, Highly stretchable and tough hydrogels, Nature 489 (7414) (2012) 133–136.
[17] C. Liu, N. Morimoto, L. Jiang, S. Kawahara, T. Noritomi, H. Yokoyama, K. Mayumi, K. Ito, Tough hydrogels with rapid self-reinforcement, Science 372 (6546) (2021) 1078–1081.
[18] R. Bai, J. Yang, Z. Suo, Fatigue of hydrogels, Eur. J. Mech. A Solids 74 (2019) 337–370.
[19] J. Tang, J. Li, J.J. Vlassak, Z. Suo, Fatigue fracture of hydrogels, Extreme Mech. Lett. 10 (2017) 24–31.
[20] R. Bai, Q. Yang, J. Tang, X.P. Morelle, J. Vlassak, Z. Suo, Fatigue fracture of tough hydrogels, Extreme Mech. Lett. 15 (2017) 91–96.
[21] E. Zhang, R. Bai, X.P. Morelle, Z. Suo, Fatigue fracture of nearly elastic hydrogels, Soft Matter 14 (18) (2018) 3563–3571.
[22] W. Zhang, J. Hu, J. Tang, Z. Wang, J. Wang, T. Lu, Z. Suo, Fracture toughness and fatigue threshold of tough hydrogels, ACS Macro Lett. 8 (1) (2018) 17–23.
[23] W. Zhang, X. Liu, J. Wang, J. Tang, J. Hu, T. Lu, Z. Suo, Fatigue of double-network hydrogels, Eng. Fract. Mech. 187 (2018) 74–93.
[24] R. Bai, J. Yang, X.P. Morelle, C. Yang, Z. Suo, Fatigue fracture of self-recovery hydrogels, ACS Macro Lett. 7 (3) (2018) 312–317.
[25] S. Lin, J. Liu, X. Liu, X. Zhao, Muscle-like fatigue-resistant hydrogels by mechanical training, Proc. Natl. Acad. Sci. USA 116 (21) (2019) 10244–10249.
[26] S. Lin, X. Liu, J. Liu, H. Yuk, H.-C. Loh, G.A. Parada, C. Settens, J. Song, A. Masic, G.H. McKinley, Anti-fatigue-fracture hydrogels, Sci. Adv. 5 (1) (2019) eaau8528.
[27] X. Li, Cui K., T.L. Sun, L. Meng, C. Yu, L. Li, C. Creton, T. Kurokawa, J.P. Gong, Mesoscale bicontinuous networks in self-healing hydrogels delay fatigue fracture, Proc. Natl. Acad. Sci. USA 117 (14) (2020) 7606–7612.
[28] X. Liang, G. Chen, S. Lin, J. Zhang, L. Wang, P. Zhang, Z. Wang, Z. Wang, Y. Lan, Q. Ge, J. Liu, Anisotropically fatigue-resistant hydrogels, Adv. Mater. 33 (30) (2021) e2102011.
[29] M. Hua, S. Wu, Y. Ma, Y. Zhao, Z. Chen, I. Frenkel, J. Strzalka, H. Zhou, X. Zhu, X. He, Strong tough hydrogels via the synergy of freeze-casting and salting out, Nature 590 (7847) (2021) 594–599.
[30] C. Xiang, Z. Wang, C. Yang, X. Yao, Y. Wang, Z. Suo, Stretchable and fatigue-resistant materials, Mater. Today 34 (2020) 7–16.
[31] H. Yang, M. Ji, M. Yang, M. Shi, Y. Pan, Y. Zhou, H.J. Qi, Z. Suo, J. Tang, Fabricating hydrogels to mimic biological tissues of complex shapes and high fatigue resistance, Matter 4 (6) (2021) 1935–1946.
[32] X. Zhao, J. Wu, Y. Zhou, Y. Pan, T. Lu, X. Song, J. Hu, Fatigue behaviors of physical hydrogels based on hydrogen bonds, Extreme Mech. Lett. 46 (2021) 101320.
[33] G. Lake, A. Thomas, The strength of highly elastic materials, Proc. R. Soc. Lond. Ser. A Math. Phys. Sci. 300 (1460) (1967) 108–119.
[34] S.J. Rowan, S.J. Cantrill, G.R. Cousins, J.K. Sanders, J.F. Stoddart, Dynamic covalent chemistry, Angew. Chem. Int. Ed. 41 (6) (2002) 898–952.
[35] J. Liu, C. Yang, T. Yin, Z. Wang, S. Qu, Z. Suo, Polyacrylamide hydrogels. II. Elastic dissipater, J. Mech. Phys. Solids 133 (2019).
[36] F.D. Osterholtz, E.R. Pohl, Kinetics of the hydrolysis and condensation of organofunctional alkoxysilanes: A review, J. Adhes. Sci. Technol. 6 (1) (1992) 127–149.
[37] Q. Liu, G. Nian, C. Yang, S. Qu, Z. Suo, Bonding dissimilar polymer networks in various manufacturing processes, Nature Commun. 9 (1) (2018) 846.
[38] C. Yang, T. Yin, Z. Suo, Polyacrylamide hydrogels. I. Network imperfection, J. Mech. Phys. Solids 131 (2019) 43–55.
[39] R.W. Ogden, Non-Linear Elastic Deformations, Dover Publications, 2013.
[40] R. Rivlin, A.G. Thomas, Rupture of rubber. I. Characteristic energy for tearing, J. Polym. Sci. 10 (3) (1953) 291–318.
[41] S. Cai, Z. Suo, Equations of state for ideal elastomeric gels, Europhys. Lett. 97 (3) (2012).
[42] T. Matsuda, R. Kawakami, R. Namba, T. Nakajima, J.P. Gong, Mechanoresponsive self-growing hydrogels inspired by muscle training, Science 363 (6426) (2019) 504–508.
[43] G. Scetta, E. Euchler, J. Ju, N. Selles, P. Heuillet, M. Ciccotti, C. Creton, Self-organization at the crack tip of fatigue-resistant thermoplastic polyurethane elastomers, Macromolecules 54 (18) (2021) 8726–8737.

[44] B. Lawn, An atomistic model of kinetic crack growth in brittle solids, J. Mater. Sci. 10 (3) (1975) 469–480.
[45] E. Orowan, The fatigue of glass under stress, Nature 154 (3906) (1944) 341–343.
[46] X. Yang, J. Yang, L. Chen, Z. Suo, Hydrolytic crack in a rubbery network, Extreme Mech. Lett. 31 (2019).
[47] G. Sanoja, X.P. Morelle, J. Comtet, C.J. Yeh, M. Ciccotti, C. Creton, Why is mechanical fatigue different from toughness in elastomers? The role of damage by polymer chain scission, Sci. Adv. 7 (42) (2021) eabg9410.
[48] D. Zheng, S. Lin, J. Ni, X. Zhao, Fracture and fatigue of entangled and unentangled polymer networks, 2021, arXiv preprint arXiv:2112.12372.